Secondary electron flight times and tracks in the carbon foil time pick-up detector

Mikko Laitinen, Mikko Rossi, Jaakko Julin, Timo Sajavaara

Dept. of Physics, P.O.Box 35, 40014 University of Jyväskylä, Finland

Corresponding author: Mikko Laitinen
Telephone : +358 400994836
Fax: +358 14 617 411
E-mail: mikko.i.laitinen@jyu.fi

Abstract:

Carbon foil time pick-up detectors used in the time-of-flight measurements of MeV energy ions have been studied in connection to time-of-flight–energy spectrometer used for heavy ion elastic recoil detection analysis. In experimental coincident TOF-E data characteristic halos are observed around light element isobars, and the origin of these halos were studied. The experimental data indicated that these halos originate from single electron events occurring before the electron multiplication in the microchannel plate. By means of electron trajectory simulations, this halo effect is explained to originate from single electron, emitted from the carbon foil, hitting the non-active area of the microchannel plate. This electron creates a secondary electron from the surface and which ends up to the microchannel plate pore, is multiplied and create now a detectable signal. Other general timing gate parameters such as wire-to-wire spacing of the grids, acceleration potential of the 1st grid and the mirror grid potential gradient were also studied in order to improve the detector performance.

Keywords:

timing gate, carbon foil time pick-up detector, Time-of-Flight, ToF-ERDA, spectrometer.

1 Introduction

Modern time-of-flight elastic recoil detection (ToF-ERD) spectrometers often use two carbon foil time pick-up detectors [1--3], similar to the design by Busch et al. [4]. This type of timing detector has typically five basic components (see Fig. 1): 1) The carbon foil that emits the electrons due to ion passage, 2) the toblerone-part which accelerates the electrons from the carbon foil and is accompanied by transparent grid, or mesh structures providing field free central region, 3) electrostatic mirror to bend the path of the electrons by 90 degrees back to the field free toblerone-part, 4) microchannel plate (MCP) for electron multiplication and 5) the anode to collect the electrons. In addition to these, the decision of using the timing gate in forward or backward direction related to the incident ion needs to be made.

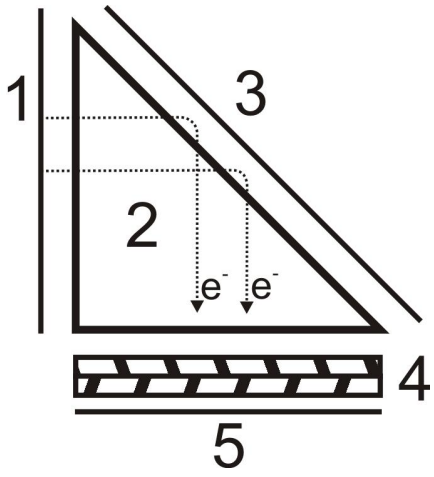

Figure 1. Basic components of the carbon foil time pick-up detector. This type of timing gate has five components: 1) carbon foil, 2) field free toblerone-part, 3) mirror grid, 4) MCP for electron multiplication and 5) anode to collect the electrons.

All of these individual detector components affect the timing performance through their material properties, structural geometry or by applied voltages. Energetic ion impact into the carbon foil will induce emission of zero to multiple secondary electrons, that can have wide energy and angular distributions [5,6]. The number of emitted electrons can be increased by other materials deposited on top of the carbon foil. These materials, such as LiF [2] or Al_2O_3 grown by atomic layer deposition (ALD) [7] can enhance the electron emission and therefore increase the detection efficiency for light ions. The emitted electrons having both the high energy and large emission angle perpendicular to the foil, can distort the timing signal already before the first accelerating grid causing non-isochronous electron transportation to the MCP. The grid spacing grid uniformity/smoothness and voltages applied to the mirror grid and toblerone-part also affect the electron trajectories before the MCP. The voltage, pore size and pore length of the MCP, and the distance between the individual MCP plates and their potential difference in chevron composition affect the rise time and width of the electron pulse [8]. Finally the anode design can have a big effect to the timing properties of the carbon foil time pick-up detectors in the time-of-flight measurements. In addition to these individual

timing gate components, the decision of using the timing gate in forward direction related to the incident beam i.e. the foil faces the beam first or in the backward geometry where mirror faces towards the incident beam, needs to be made as well.

In this paper we focus on the timing pulse properties of the single carbon foil time pick-up detector. Main emphasis is given to the individual parts before the MCP and how the different grid designs can affect the electron flight time properties from the carbon foil to the MCP. An explanation to the halo effect typically seen also in other studies [9,10] around the hydrogen events in the ToF-E histograms is proposed. The MCP and anode part are left for less attention as ready MCP solutions with fast rise times (down to 300 ps in standard products [8,11]) and matched anodes can be acquired commercially by several suppliers. For the case of timing gate orientation, one can for example win few centimeters in the ToF length if the first timing detector is facing forward and the second in backward electron emission direction. The forward direction can also produce more electrons due to the ion impact but their energy and especially their angular distribution is not that favorable than in the backward direction, according to the data in [6]. The angle and energy distributions of electrons and their effect to the timing properties are discussed in more detail in the following.

2 Experimental and simulation parameters

ToF-ERDA spectrometer with two carbon foil time pick-up detectors is located at the +15 degree beam line of the 1.7 MV Pelletron accelerator of the Accelerator Laboratory, University of Jyväskylä. ToF-ERDA method is best suited for light elements on heavy substrates, but the hydrogen recoils are often the most difficult ones to detect. One reason for this is the small stopping force of the detector carbon foils for hydrogen. Due to this, only a very small number of electrons is emitted from the carbon foil by the passing hydrogen ion. The single electron events are studied as a cause for the halos observed in the hydrogen isobars. The halos were experimentally studied with 2 MeV $^{1}H^{+}$ beam scattered from a thick target. The model system in the simulations was the second timing gate.

2.1. Timing gates of the ToF-ERDA spectrometer

The first (T1) and second (T2) timing gates are not identical in our system. The main differences are the physical sizes and the voltages of the different individual components.

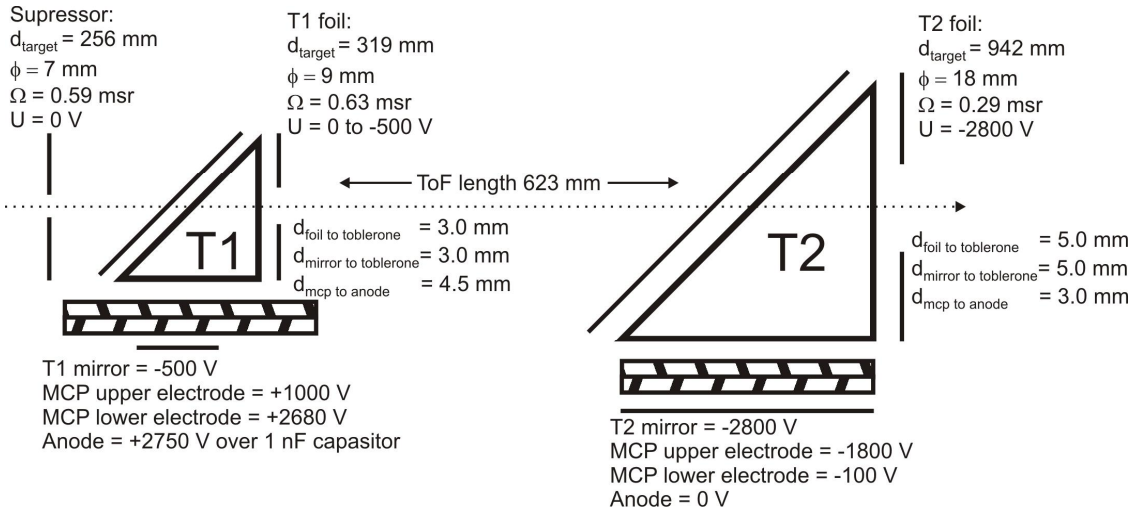

Figure 2. Distances, carbon foil sizes, solid angles and voltages of the Jyväskylä ToF-ERDA timing gates.

The measures and voltages of the TOF telescope are shown in Fig. 2. The T2 has a solid angle of 0.29 msr, roughly half of the T1, although it is physically considerably larger. The total solid angle of the ToF-E telescope is governed by the T2 carbon foil holder (see also Fig. 3 b) as the silicon energy detector, placed right after the T2, has larger surface area of 450 mm^2. The same MCP's (>40 mm active area, 12 μm pore size, d/L=1:40) are used in both of the timing gates. The anodes in both timing gates are modified from the original MCP stack-structure and are currently made from a printed circuit board. Anode to MCP electrode distance is 4.5 mm and 3.0 mm for the T1 and T2, respectively. Supplier for the MCP's was Tectra [11].

The used voltages are different for T1 and T2. In the T1 the anode is at +2750 V, MCP lower (closer to anode) and upper electrodes are at +2660 V and +1000 V respectively, and the carbon foil can be grounded or slightly negatively biased. The T1 mirror grid needs to be negatively biased as it otherwise would accelerate free electrons towards the grid and the MCP; typically -500 V is used in our measurements. The signal is taken from the T1 anode over a 1 nF capacitor. For T2 -2800 V is applied on both mirror and foil, -1800 V on MCP upper electrode and on toblerone-part and anode is at ground potential.

High transparency grids in our timing gates compose of thin (diameters 25 and 20 μm) Au plated tungsten wires [12] that are point welded to their support frames (see Fig.3 a). The wire-to-wire spacing is 1.0 mm which was adopted from the timing gates developed earlier in our lab for nuclear physics experiments [13,14]. Distances from the foil to the first accelerating grid are 3.0 mm and 5.0 mm for T1 and T2, respectively. The distances of the mirror grids from the toblerone grids are the same than those of the foils. By using this type of point welded grid structure we have achieved better than 86 % optical transmission through two timing gates (6 wire grids in total) together with the highly parallel and well aligned grid structure.

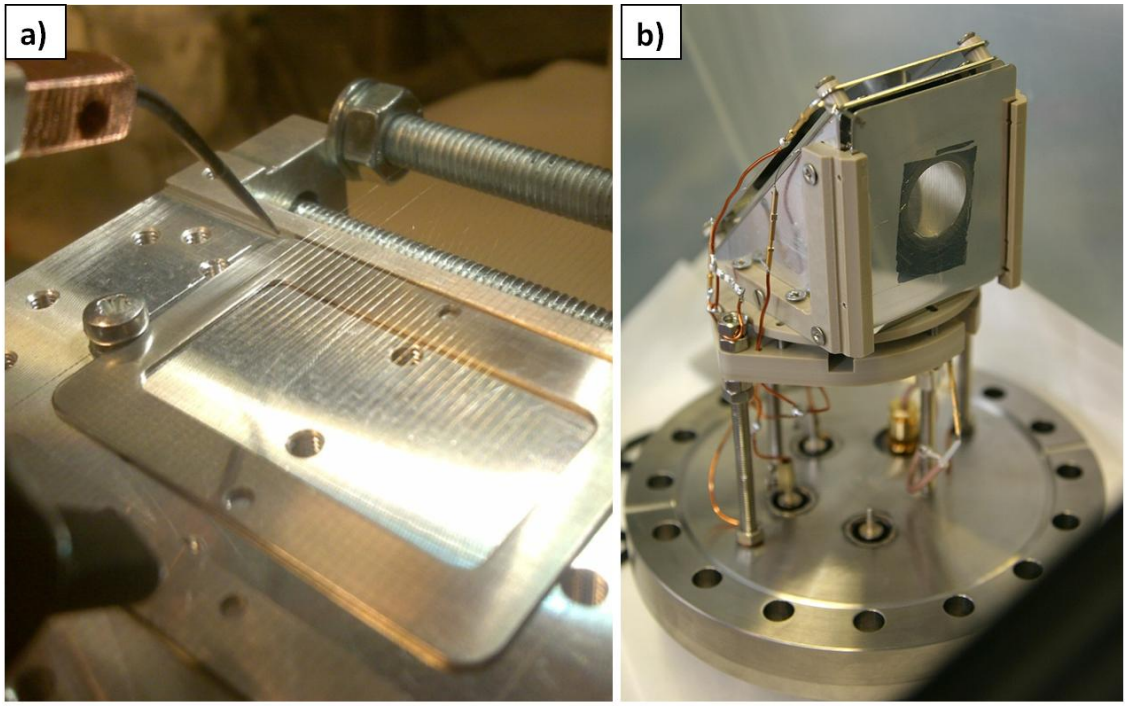

Figure 3. a) Point welding jig used in the fabrication of a grid. Wire (here 20 µm) is first wound around the jig where the pitch is determined by the pitch of the threads in both ends. Then, each wire is point welded from both ends to the frame holding the final grid structure. b) T2 timing detector fully assembled with 10 µg/cm^2 carbon foil.

2.2. Electron flight time and -path simulation at the timing gate

A 2D model of the T2 timing gate was brought to the Simion program [15]. Simion is a software package primarily used for calculating electric fields and the charged particle trajectories in those fields [15].

Physically larger T2 was selected for the simulations as electron flight times, and possible time spreads were expected to be larger in it. Possible results were expected to scale down for the smaller T1. The model of the T2 timing gate had 20 000 × 20 000 pixels so that one pixel corresponded to about 3.5 µm. Thus 25 µm wires in the real system had diameter of 7 pixels in the simulations.

The focus in the simulations was to find the optimal wire-to-wire spacing and potentials for the best achievable isochronous electron transport from the foil to the MCP electrode. The wire-to-wire spacing was varied from the ideal case (transparent, flat electric potential field) to 0.5 mm, 1.0 mm, 1.5 mm and 3.0 mm. During the selection of the initial standard parameters for electron emission values, which was a sort of a compromise of the literature data available, mainly values from the Ref. [6] was finally used. The standard electron emission parameters were kept as: E_{kin} = 4 ± 4 eV (Gaussian distribution) and incident angle of electron emission was uniformly distributed ± 30º from the normal of the foil surface. The potentials were nominally the same as in the

experimental configuration. Also other electron emission parameters from the carbon foil were studied to cover wider electron energy and angular distributions and to verify their effect to the electron flight times compared to the standard electron emission parameters.

In other simulations the electron scattering from the wire grids and from the MCP upper electrode was studied in order to find the explanation to the longer than average electron flight times seen in the experimental spectrum. The electron coming from the carbon foil has energy about 1000 eV when hitting the wires or the MCP electrode. A single secondary electron was created from the single impact and the emission direction was set as a specular reflection (incident angle = reflection angle). Estimation of the created secondary electron kinetic energy and the detection probability at the MCP pore was problematic. Experimental data for the secondary and backscattering electron energies and probabilities used in these simulations were taken from [16,17]. A function fitted to the data shown in Fig. 4 a) was used by a random generator to determine the SE emission energy after the initial impact. However, the data points in Fig. 4 a) were taken directly from the Ref. [16] and are for the 550 eV incident impact energy. Although the energy data for incident electron reach only 550 eV at [16] and not 1000 eV it can be concluded from [16] and [17] that most of the secondary electrons are always emitted with low energies <20 eV, having an intensity maximum at around 2 eV. This is regardless of the impact energy. When going to higher energies the secondary electron emission intensity drops close to zero for energies above 50 eV. However, there is always a small amount of true backscattered/reflected electrons which have nearly the same energy as the incident particle but their probability at 550 (and 1000) eV is very small. For this reason we have neglected the material differences between [16] and our system (Cu at [16] vs. Au plated W at wire grids and Ni at the MCP electrode material).

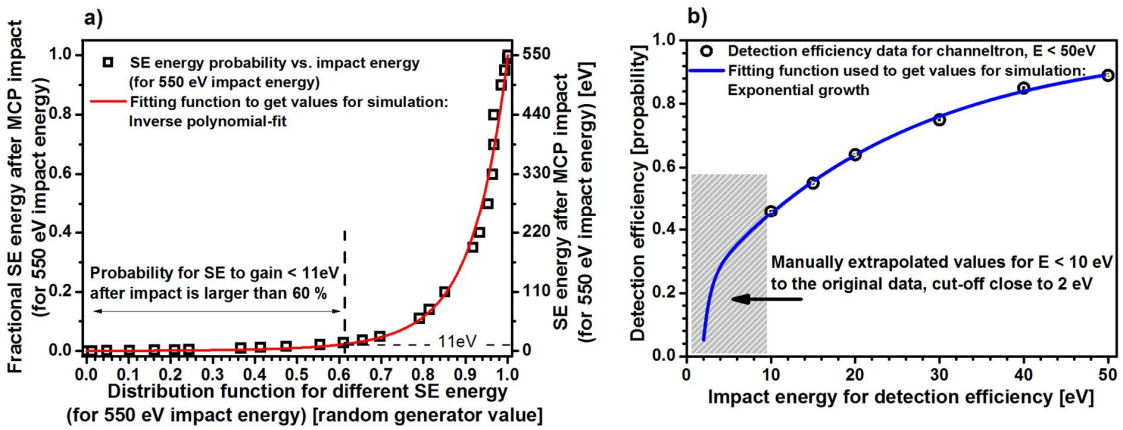

Figure 4. a) The secondary electron emission energy distribution as a distribution function (probability) and b) MCP detection efficiency vs. electron impact energy. The probability function in a) was used to calculate the energy for the emitted electron after the primary electron had hit to the wire or the MCP surface. About 60 % of these secondary electrons had less than 11 eV (= 0.02 × 550 eV) energy although small amount of the emissions occurred almost at impact energies (true backscattering events). In b) estimated values for the detection efficiency of the MCP were taken from Ref. [49] down to 10 eV and the points below the 10 eV impact energy are approximated with a cut-off value of < 2 eV. Higher than 50 eV impact energies were assumed to have constant detection efficiency (~90 %) in the simulations.

The energy distribution of the secondary electrons (from the MCP electrode) influences not only the electron flight time distribution before the MCP but also the detection efficiency of the MCP. The detected hydrogen yield can be greatly affected by the MCP detection efficiency for low energy electrons. The MCP detection efficiency for our configuration was not available for very low electron energies. An approximation for the MCP detection efficiency at smallest energies was obtained partly (down to 10 eV) from [18] and is shown in Fig. 4 b).

3. Results

3.1. Electron paths and flight times: the effect of the grids and voltages

Both wire-to-wire spacing and the applied foil, toblerone part and mirror grid voltage affect the electron transport from the foil to the MCP surface. Visual examples are presented in the Fig. 5. Here a) to c) represent different wire spacings (and also mirror grid distance change in c) which illustrate the need for obtaining both smooth acceleration from the foil to the 1st grid and a field free region inside the toblerone-part. The voltage configuration can affect the isochronous transportation of electrons and also the position information of the electron impact location on the MCP. This is demonstrated in Fig. 5 d) to f) where the time scale (200 ps ticks) is visualized by green markers.

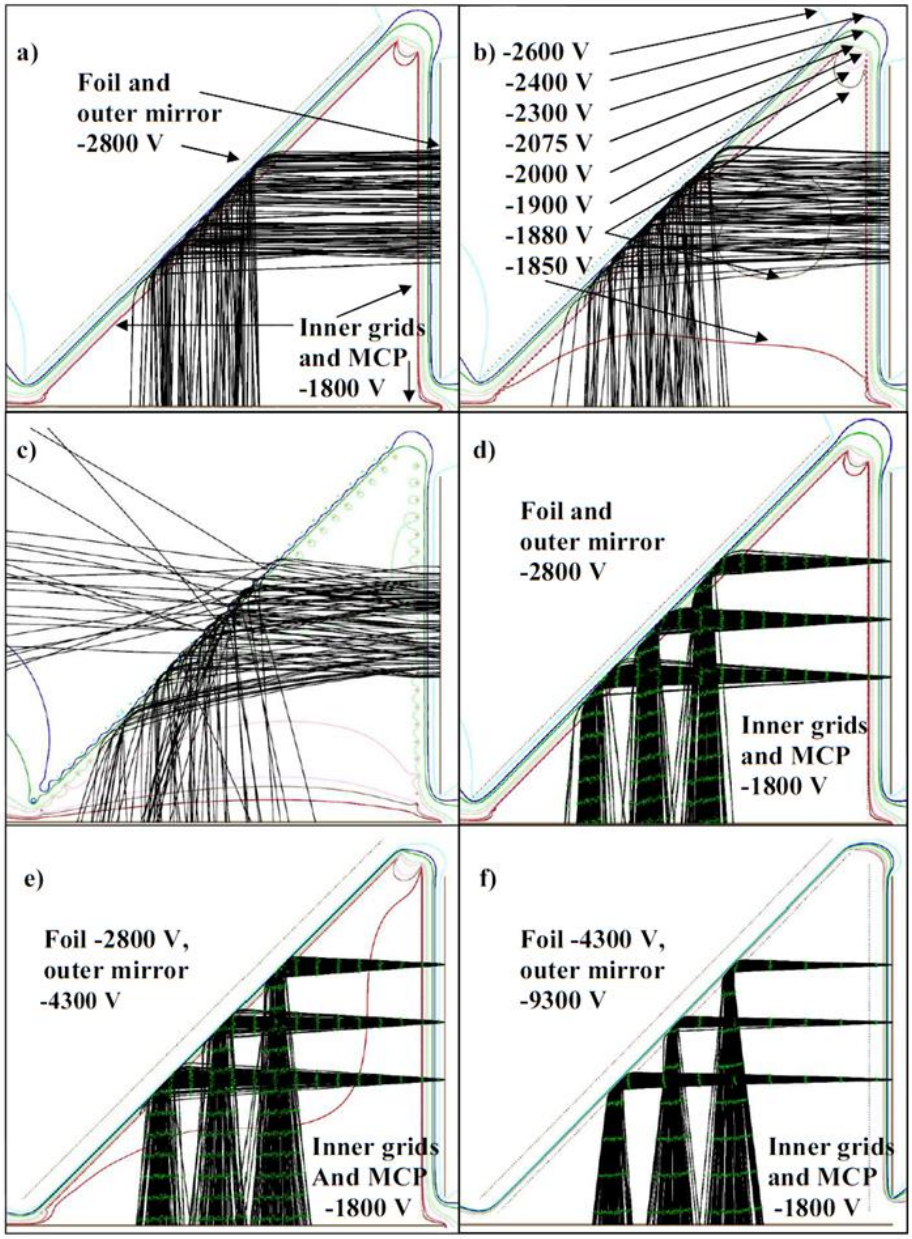

Figure 5. Electron trajectory simulations made with SIMION program for the T2 timing gate with different wire-to-wire spacings and applied voltages. In a), b) and c) the wire-to-wire spacings are 0.5 mm, 1 mm and 3 mm, respectively, where b) represents the experimental configuration in Jyväskylä. In c) the outer mirror grid is brought 1/3 closer to the inner mirror grid from the original perpendicular distance of 5.0 mm. In d), e) and f) the accelerating foil potential and the outer mirror potential has been changed for the 0.5 mm wire-to-wire spacing –case. The (green) markers on the black electron paths indicate 200 ps time intervals. In these simulations, all electrons emitted from the foil have initial energy of (4 ± 6) eV with uniform distribution of ± 40 degree perpendicular to the foil surface (note: these emission values are slightly different than the standard electron emission parameters used elsewhere in this paper).

In general, the larger the individual wire-to-wire spacing is, the greater is the spreading of the electron tracks. To reduce the electron track and electron flight time spread, one should use small wire-to-wire spacing particularly in the 1st accelerating grid. To further reduce the electron flight time spread, the potential difference between mirror grids should be about 2 to 2.5 times higher than the potential difference from the foil to the 1st accelerating grid (see Fig. 6 b). The high mirror grid potential reduces the time the electrons spend in the mirror volume and thus reduces the deviation in the lengths of the electron flight paths. This path length deviation is originally caused by the non-uniform entering angle to the mirror volume. However, as seen from the Fig. 6 b), one cannot increase the mirror voltage infinitely to reduce the flight time spread as when the electrons are pushed too close to the toblerone wire grid their flight times start to deviate from the shortest achievable value. This does not happen for the ideal grid because this spread originates from the influence of the individual wire potentials of the non-ideal grid to the electron flight paths.

One can reduce the electron flight time by increasing the acceleration potential and this also reduces the electron flight time spread (Fig. 6 a). The spread almost saturates for acceleration potentials above 1000 V. Very high potential differences between the foil and the toblerone can quickly lead to practical problems like bulging of the carbon foil due to electric field or sparking, and it will clearly make the tandem effect [19] larger in the case of T1, especially if the foil is in high potential and not grounded.

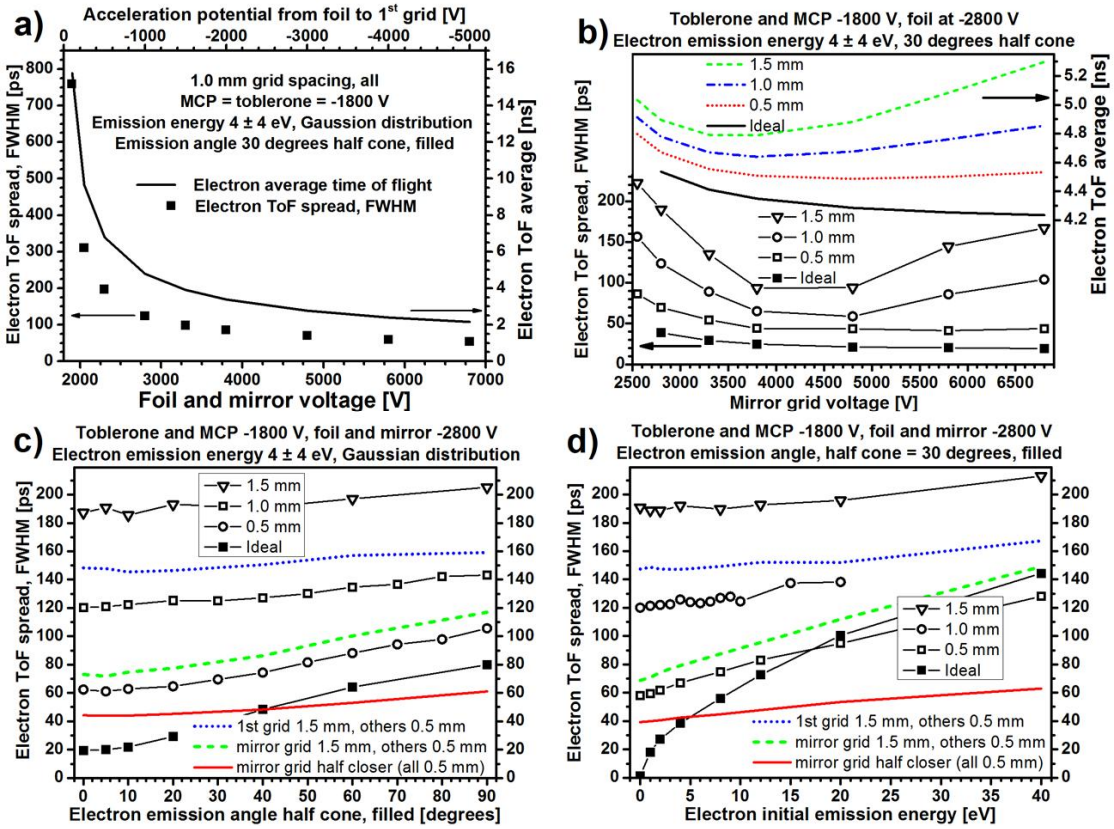

Figure 6. The effect of different timing gate and electron emission parameters to the electron flight time spread. a) The electron ToF spread and the electron flight times as a function of foil and mirror voltage. b) The TOF spread as a function of mirror grid potential for a fixed foil voltage. The TOF spread as a function of electron emission half cone c) and electron emission energy d).

Simulation results shown in the Fig. 6 c) and d) confirm that those electrons having the highest energy and widest emission angle when exiting the carbon foil will result the greatest time spread in electron flight times. While these events cannot be avoided, it is possible to minimize the timing spread caused by these electrons by design. Having as small wire-to-wire spacing as possible in the first acceleration grid, electric field strength in the mirror about two times as high as in the accelerating grid, one can still save some effort during the grid construction if having only 1.5 mm wire-to-wire spacing in the outer mirror grid. As our simulations indicate that, our current wire-to-wire spacing and used voltages in the timing gates are not optimal when electron flight time spread is concerned. By reducing the current 1.0 mm wire-to-wire spacing to 0.5 mm and by increasing the current mirror voltage from -2800 V closer to -4000V for T2 one can reduce the estimated electron flight time spread from 125 ps to less than 50 ps (taken from Fig. 6 b)) without touching the foil or MCP/toblerone voltages.

The impact of the electron flight time spread in the single timing gate to the actually measured ion ToF spread in the two timing gates is not linear. It can be estimated that for

the heavier ions, which emit more electrons when passing through the carbon foils, the spread of electrons flight times have smaller effect to the ion time-of-flight spread. This is due to more uniform electron emission cone at the carbon foil and because the fastest electrons will always cause the initial signal rise at the anode after the MCP. However, the lighter ions such as hydrogen to carbon which emit only one (even zero) to few electrons from the carbon foil, the single electron flight time is more important. This is because if the only emitted electron(s) flew the shortest and the longest flight times before the MCP in the T1 and T2, respectively, a larger spread for the ion ToF will be measured. If compared to the other effects [3,20] causing the measured ion ToF spread, including the straggling in the first carbon foil, the overall contribution of the electron flight time spread in a single time gate is small. If for example timing resolution cannot be pushed down to 150 ps regime (corresponding about 30 keV for 4 MeV ions for Jyväskylä ToF-ERDA [21]) and the kinematic effect due to large solid angle cannot be compensated, the electron flight time spread is very small compared to other sources of ion ToF spreads.

3.2. Halo around the hydrogen time-of-flight events

Measured ToF-E isobars for the hydrogen have a clearly structured halo on both longer and shorter time-of-flights (see Fig. 7). For hydrogen these halo events can contribute at high energies up to 25 % of all hydrogen events compared to the tight selection (see Fig. 7). Although this type of halo is most pronounced for the hydrogen, similar halos but with reduced intensity can also be seen up to mass of carbon. The halo is typically about ±15 ns wide from the center of the as-expected ToF-value. By varying both the MCP and the foil (and mirror) voltages as shown in Fig. 7 it can be deduced that the events that give birth to the halo are generated after the foil and before the MCP. As seen in Fig. 7 b) the T2 foil voltage reduction (nominally -1000 V compared to the MCP upper surface electrode) also spreads out the halo to the right side, longer ToF, but not completely smooths it out. The Fig. 7 c) and d) on the other hand indicate that the halo is generated from those events that have longer than normal ToF and especially from those events that have smaller than average pulse height as they vanish earlier with smaller MCP voltages (gain) compared to the main peak intensity. This pulse height difference in the halo and the main peak was also confirmed with the fast CAEN N6751 digitizer unit with full signal shape recording. From the Fig. 7 b) it is also more evident that there is a small gap between the halo-events and the main peak in which less events are detected. This shallow event free gap is more clearly visible in Fig. 9.

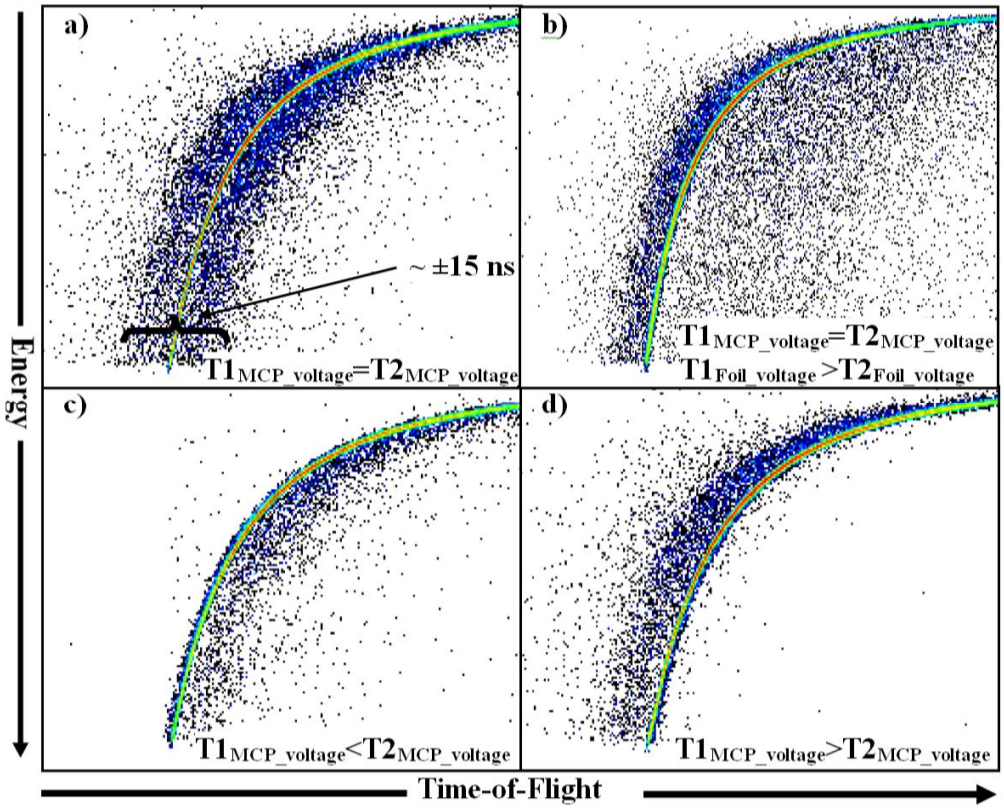

Figure 7. Time-of-flight−energy histogram showing the influence of the MCP voltage and foil voltage to the scattered hydrogen ion TOFs. When operating at nominal voltages for our system, hydrogen has a clear background distributing over ±15 ns from the main isobar as well as lighter background spreading further away as shown in a). In b) only the T2 foil has reduced voltage and therefore only smaller electron energies are available within the T2. In c) only T1 MCP gain has been lowered so that only multiple electron events generate detectable signals at T1 (similarly for T2 in d).

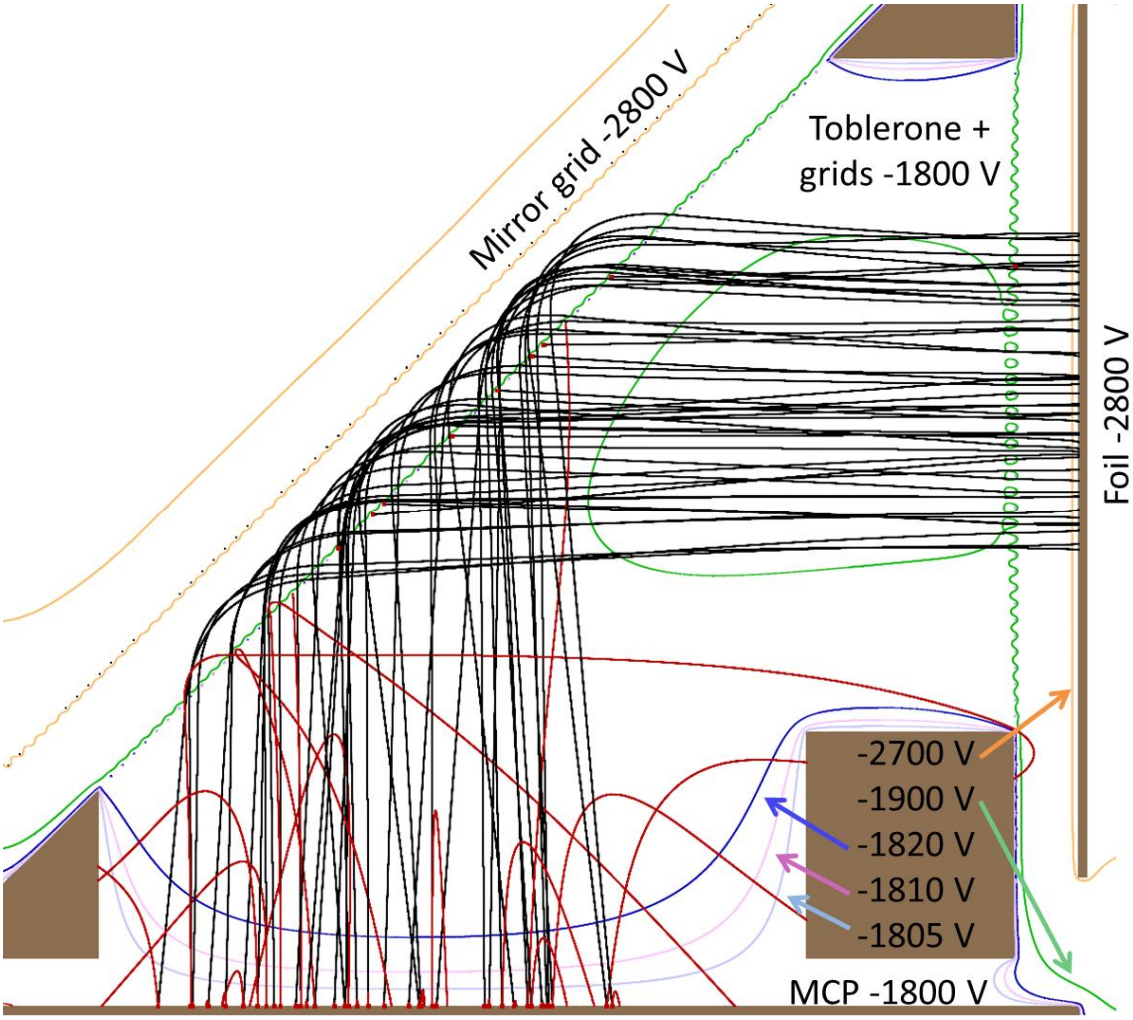

Figure 8. Electron paths (43) in our current T2 timing gate simulated with nominal parameters. Single secondary electron emission was set to occur due to the primary electron impact. About half of the secondary electrons (48 in total) from the MCP have too little energy to be visible in this scale. In total, 10 secondary events end up to the toblerone side mirror grid and 5 to the walls of the toblerone block, while majority of the secondary electrons from the MCP surface end up back to the MCP surface and can generate a signal.

Figure 8 shows simulated electron trajectories in a timing gate. In Fig. 8 most of the secondary electron paths are not even visible and do not reach the -1805 V equipotential line above from the MCP as SE energy distribution intensity maximum is smaller than 5 eV. For the same reason most of the SEs created by the primary electron hitting the wire grids cannot escape the potential field of the individual wire.

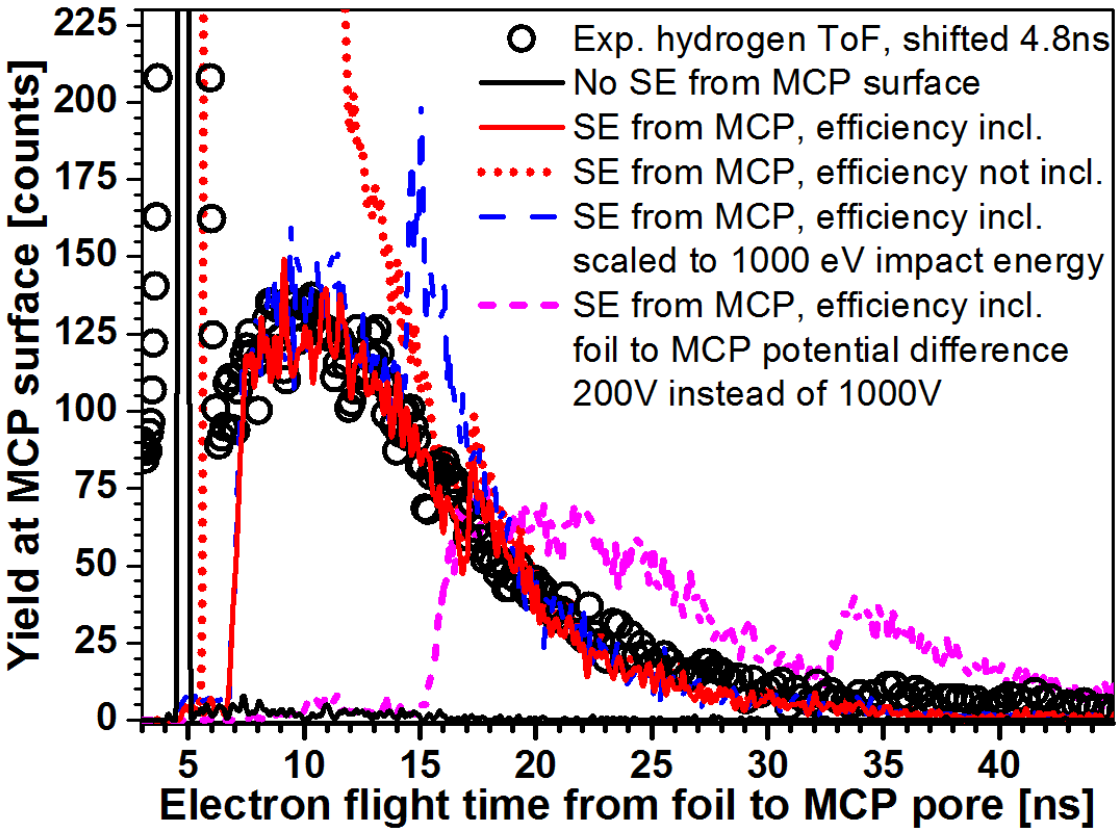

Figure 9. Experimental time-of-flight data from the hydrogen ions and corresponding electron flight time simulations from the carbon foil to the MCP surface in our current T2 detector. The use of 1000 eV impact energy instead of 550 eV changes very little the overall shape of the extended flight times with the exception of the shifted peak which is present at the simulations (see text). The solid black line represents the case in which scattering/secondary events only from the wire grids are considered. The dashed pink line shows the extended electron flight times for reduced foil and mirror potentials. In the experimental data the main peak (at 4.8 ns) has about 75 % of all events detected.

In the Fig. 9 are shown both the experimental data and simulated electron flight times in different cases. The experimental data in Fig. 9 is shifted +4.8 ns which corresponds the simulated, as-expected, electron flight time from the foil to the MCP. As seen from the Fig. 9 only a very small contribution comes from the events that have scattered only from the wires and scattering from the MCP surface dominates. The case in wich MCP detection efficiency for different energies is not included (pointed line) the electron flight times between 6 and 15 ns are considerably pronounced compared to the experimental data. However, if the MCP efficiency estimation for low electron energies is included, the yield for the shortest secondary electron flight times between 6 and 15 ns drops considerably, and simulations agree with the experimental data. There is, however, a small peak in the simulation data at about 17 ns (and a larger peak at ~15 ns for impact energies scaled to 1000 eV). The origin of this extra peak, which changes very little the overall shape of the extended flight times, is due to the highest energy electrons which

have emitted from the MCP surface. The high energy electrons, most likely backscattered ones, have enough energy to wiggle back to the mirror and foil grids in the toblerone-part before ending back to the pore of the MCP. As this type of peak is not seen in the experimental data it can be concluded that the high energy backscattering yield is overestimated in the simulation parameters. If voltage of 200 V is used for both foil and mirror instead of 1000 V, the simulated distribution of secondary electrons (Fig. 9) becomes much broader. The same effect is visible in Fig. 7 b) where roughly the same parameters were in use in an experiment.

4 Conclusions

Electron transport properties in the carbon foil time pick-up detectors, being in use in the Jyväskylä ToF-ERD setup, have been investigated. Experimentally detected halo around the hydrogen isobar in the ToF-E histogram could be reproduced by simulations and its origin is understood. Experimentally it was confirmed that the halo events had smaller MCP pulses indicating that they originate from single electron events. In the simulations the halo was confirmed to form from those secondary electrons from the MCP surface that ended up to the active MCP pore after a short time period.

More simulations were made to study the different wire-to-wire spacings and voltages in the grids for electrons with different incident energy and angle. By decreasing the wire-to-wire spacing and increasing the acceleration potential together with the mirror voltage, smaller flight time spreads were observed. By using less tightly spaced mirror grids (1.5 mm spacing), 0.5 mm spaced toblerone grids and 2–2.5 higher mirror potential difference than for the acceleration the timing spread reduces considerably.

Acknowledgements

This work was supported under the auspices of Finnish Centre of Excellence Programme 2006-2014 (Project No. 213503, 251353 Nuclear and Accelerator Based Physics), Finnish Funding Agency for Technology and Innovation (Tekes) project ALEBOND (decision no. 40079/08), MECHALD (decision no. 40207/11) and HIUDAKE (decision no. 70027/11) and Tekes EU-regional funds project (decision no. 70039/08).

References

[1] C. Kottler, M. Döbeli, F. Glaus, M. Suter, Nucl. Instr. and Meth. B, 248 (2006), p. 155.

[2] Z. Siketić, I.B. Radović, M. Jakšić, Nucl. Instr. and Meth. B, 266 (2008), p. 1328.

[3] S. Giangrandi, T. Sajavaara, B. Brijs, K. Arstila, A. Vantomme, W. Vandervorst, Nucl. Instr. and Meth. B, 266 (2008), p. 5144.

[4] F. Busch, W. Pfeffer, B. Kohlmeyer, D. Schüll, F. Pühlhoffer, Nucl. Instr. and Meth., 171 (1980), p. 71.

[5] M. Burkhard, H. Rothard, C. Biedermann, J. Kemmler, K. Kroneberger, P. Koschar, O. Heil, K. Groeneveld, Phys. Rev. Lett., 58 (1987), p. 1773.

[6] C.G. Drexler and R.D. DuBois, Phys. Rev. A, 53 (1996), p. 1630.

[7] M. Leskelä and M. Ritala, Thin Solid Films, 409 (2002), p. 138.

[8] Hamamatsu, *MCP & MCP assembly - selection guide*, http://www.sales.hamamatsu.com/resources/pdf/etd/MCPassy_TMCP0001E09.pdf (25.2.213).

[9] S. Giangrandi, *Low-energy Elastic Recoil Detection and Ion Beam Analysis for quantitative elemental profiling of thin films* (KU Leuven, 2010) PhD thesis.

[10] T. Sajavaara, *Heavy ion recoil spectroscopy of surface layers* (University of Helsinki, 2002) PhD thesis.

[11] Tectra, *Microchannel Plates and Microchannel Plate Detectors*, http://www.tectra.de/MCP.htm (25.2.1013).

[12] Luma-metal, *Gold Plated Tungsten Wire*, http://www.luma-metall.se/products/gold-plated-tungsten-wire (25.2.2013).

[13] W. Trzaska, V. Lyapin, V. Maslov, Nucl. Instr. and Meth. B, 197 (2002), p. 288.

[14] W. Trzaska, V. Lyapin, T. Alanko, M. Mutterer, J. Räisänen, G. Tjurin, M. Wojdyr, Nucl. Instr. and Meth. B, 195 (2002), p. 147.

[15] Simion 8.1, SIMION® Ion and Electron Optics Simulator, Scientific Instrument Services, Inc.

[16] V. Baglin, I. Collins, O. Gröbner, B. Henrist, N. Hilleret, and G. Vorlaufer, in *Proc. Int. Workshop on Two-Stream Instabilities in Particle Accelerators and Storage Rings, KEK*, (2001).

[17] B. Henrist, N. Hilleret, M. Jimenez, C. Scheuerlein, M. Taborelli, and G. Vorlaufer, in *proceedings of ECLOUD, Geneva, 15-18 April 2002* (CERN Report CERN-2002-001, 2002), p. 75.

[18] F. Bordoni, Nucl. Instr. and Meth., 97 (1971), p. 405.

[19] M. Döbeli, R. Ender, V. Liechtenstein, D. Vetterli, Nucl. Instr. and Meth. B, 142 (1998), p. 417.

[20] S. Giangrandi, K. Arstila, B. Brijs, T. Sajavaara, A. Vantomme, W. Vandervorst, Nucl. Instr. and Meth. B, 261 (2007), p. 512.

[21] Laitinen M., Rossi. M., Julin J., T. Sajavaara, *Time-of-flight – energy spectrometer for elemental depth profiling - Jyväskylä design*, Submitted to Nucl.Instr.and Meth.B(2013).

[22] Laitinen M. and T. Sajavaara, *Trajectory bending and energy spreading of charged ions in time-of-flight telescopes used for ion beam analysis*, Accepted to Nucl.Instr.and Meth.B(2014).